

## Supporting Information

# Fibrous mesoporous polymer monoliths: macromolecular design and enhanced photocatalytic degradation of aromatic dyes

*Ji Ae Chae,<sup>a</sup> Songah Jeong,<sup>a</sup> Hea Ji Kim,<sup>a</sup> Tomohiro Tojo,<sup>b</sup> Yuree Oh,<sup>a</sup> Won Seok Chi,<sup>a</sup>  
Hyeonseok Yoon,<sup>a</sup> and Hyungwoo Kim<sup>\*a</sup>*

<sup>a</sup> School of Polymer Science and Engineering & Alan G. MacDiarmid Energy Research Institute,  
Chonnam National University, 77 Yongbong-ro, Buk-gu, Gwangju 61186, Korea

<sup>b</sup> Department of Electrical and Electronic Engineering, Faculty of Science and Technology, Shizuoka  
Institute of Science and Technology, 2200-2 Toyosawa, Fukuroi, Shizuoka 437-8555, Japan

Corresponding author e-mail: kimhw@jnu.ac.kr

## Table of Contents

Materials .....	S-1
Characterization .....	S-1
Synthetic Procedures .....	S-2
Supplementary Figures and Graphs.....	S-3
NMR and HRMS Spectra.....	S-8
References .....	S-9

## Materials

1,3,5-Triethynyltriphenylbenzene (**1**) was synthesized as reported by Galanti et al.<sup>S1</sup> (Z)-2,3-Bis(4-iodophenyl)acrylonitrile (**2**) was synthesized as reported by Chen et al.<sup>S2</sup> The control film (CF3) with 1,3,5-triethynylbenzene (**4**) and **2** was synthesized as reported by Chae et al.<sup>S3</sup> 4-Bromoacetophenone, trifluoromethanesulfonic acid, 1,3,5-tris(4-bromophenyl)benzene, ethynyltrimethylsilane, 4-iodophenylacetonitrile, 4-indobenzaldehyde, ethynylbenzene, basic green 1 (>99%), rhodamine 6G (>99%), and triethylamine were purchased from TCI. 1,4-Diiodotetrafluorobenzene, 1,4-diiodobenzene (**5**), PdCl<sub>2</sub>(PPh<sub>3</sub>)<sub>2</sub> (>99%), copper(I) iodide (CuI, >99%), methylene blue (>99%), tetrahydrofuran (THF), acetonitrile, and toluene were purchased from Sigma-Aldrich. Other common solvents such as methanol (MeOH), dichloromethane (DCM), hexanes and acetone were purchased from DaeJung. All other reagents used were purchased commercially and used as received unless otherwise noted. All chemicals were analytical grade and used without any further purification.

## Characterization

Proton nuclear magnetic resonance (<sup>1</sup>H NMR) spectra were recorded using MestReNova 400 MHz NMR spectrometers at 25 °C. Proton chemical shift are expressed in part per million (ppm, δ scale) and are referenced to tetramethylsilane ((CH<sub>3</sub>)<sub>4</sub>Si 0.00 ppm) or to residual protium in the solvent (CDCl<sub>3</sub>, δ 7.26 ppm). Data are represented as follows: chemical shift, multiplicity (s = singlet, d = doublet, t = triplet, q = quartet, m = multiplet and/or multiple resonances, br = broad peak), integration, and coupling constant (*J*) in hertz. Carbon nuclear magnetic resonance (<sup>13</sup>C NMR) were recorded using Bruker 400 MHz NMR spectrometers at 25 °C. Carbon chemical shifts are expressed in parts per million (ppm, δ scale) and are referenced to the carbon resonances of the NMR solvent (CDCl<sub>3</sub>, 77.23 ppm).

High-resolution mass spectrometry (HRMS) was performed using a JMS-T200GC (JEOL USA, Inc., Peabody, MA) time-of-flight mass spectrometer in a field desorption mode (Waters, Milford, MA).

Nitrogen adsorption–desorption isotherms were measured at 77 K by using a Belsorp-Max (BEL Japan, Inc.) apparatus. Samples were degassed at 50 °C under vacuum for at least 12 h before measurements, and ultra-high purity grade nitrogen gas was used for all measurements. The specific surface area was calculated by Brunauer–Emmett–Teller (BET) method and the pore size distribution was estimated according to the nonlocal density function theory (NLDFT) with a slit model. Total pore volumes were calculated at a relative pressure of P/P<sub>0</sub> = 0.990.

Uniaxial compressive tests were performed using a universal testing machine (UTM) (MCT-2150, A&D, Japan) with a 500-N load cell at 25 °C in air. Tensile samples for the mechanical testing were glued between two slide glass with a superglue for the measurement. The samples were elongated at a rate of 10 mm min<sup>-1</sup> until broken and triplicated. Then, stress–strain curves were recorded. The cylindrical samples were compressed at a rate of 10 mm min<sup>-1</sup> and triplicated during the measurement. Then, stress–strain curves were recorded. Young's modulus was obtained from the initial slope of the stress–strain curve in the strain range of 0–10%.

Morphology was observed using a Carl Zeiss SUPRA 55VP scanning electron microscope (SEM) at an accelerating voltage of 2 kV. Before the measurement, the sample was dried in vacuum and coated with a thin platinum layer.

Photoluminescence spectra were measured using a Shimadzu RF-5301PC spectrofluorometer.

Attenuated total reflectance Fourier-transform infrared spectroscopy (ATR-FTIR) was performed using Thermo Scientific Nicolet 6700 was used to observe absorption spectra of film and powder.

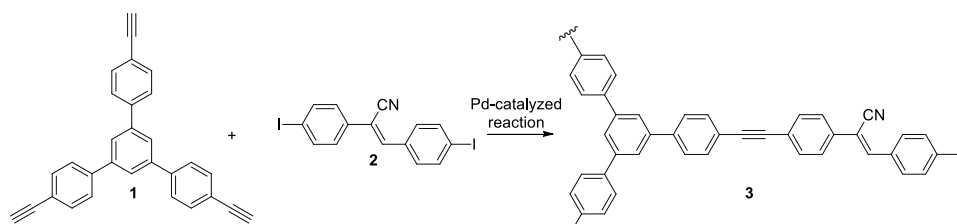
Water Contact angle measurements were conducted using a SurfaceTech GSA-X goniometer at 25 °C in air. The contact angle measurement was performed on a flat surface. The angles were measured immediately after dripping a water droplet on the surface of sample.

Solid-state  $^{13}\text{C}$  NMR spectra were obtained with a Bruker Avance II spectrometer (500 MHz) equipped with a cross-polarization–total sideband suppression (CP/TOSS) probe.

UV-Vis spectra were observed by an Optizen 2120 UV spectrophotometer with a plastic cuvette with a 10-mm path length.

## Synthetic Procedures

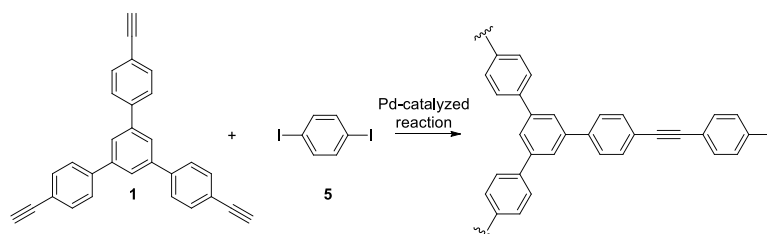
### Synthesis of powdery **3**



**Scheme S1.** Synthetic procedure for **3**.

*Agitated condition:* To a solution of **1** (37.9 mg, 0.1 mmol, 1.0 equiv), **2** (45.7 mg, 0.1 mmol, 1.0 equiv) and bis(triphenylphosphine)palladium(II) dichloride (2.11 mg, 3.3  $\mu\text{mol}$ , 0.03 equiv) in 1:1 PhMe–THF (2.65 mL, v/v) was added a solution of copper(I) iodide (0.57 mg, 3.3  $\mu\text{mol}$ , 0.03 equiv) in triethylamine (0.75 mL). After stirring vigorously at 25 °C for 24 h, the resulting powder was filtered and washed with MeOH, THF, and acetone, consecutively. The product was further purified by gentle stirring in MeOH for another 24 h and dried under vacuum at 25 °C to afford **3** as a yellow powder (39.3 mg; Yield, 67.9%).

### Syntheses of control networks



**Scheme S2.** Synthetic procedure for the control network with **5**.

*The control network with **1** and **5** (CF1):* To a control sample solution of **1** (66.9 mg, 0.117 mmol, 1.0 equiv), 1,4-diodobenzene (**5**) (58.3 mg, 0.177 mmol, 1.0 equiv), and bis(triphenylphosphine)palladium(II) dichloride (3.72 mg, 5  $\mu\text{mol}$ , 0.03 equiv) in 7:1 toluene–acetonitrile (0.53 mL, v/v) was added a solution of copper(I) iodide (1.52 mg, 8  $\mu\text{mol}$ , 0.03 equiv) in triethylamine (0.265 mL). The monolithic product was obtained from a mould under the non-agitated conditions. After storing at 25 °C for 24 h without agitation, the resulting polymer was filtered and washed with MeOH, THF, and acetone consecutively. The obtained product was further purified by gentle stirring in MeOH for another 24 h and dried under vacuum at 25 °C to afford the desired yellow monolith (76.3 mg; Yield, 95.6%).

*The control network with **1** and a 1:1 mixture of **2** and **5** (CF2):* This sample was synthesized as following the similar manner described above except for using a 1:1 mixture of **2** and **5**. Quantities are **1** (37.9 mg, 0.1 mmol, 1.0 equiv), **2** (22.9 mg, 0.05 mmol, 0.5 equiv), **5** (16.5 mg, 0.05 mmol, 0.5 equiv). (65 mg; Yield, 76.2 %).

## Supplementary Figures and Graphs

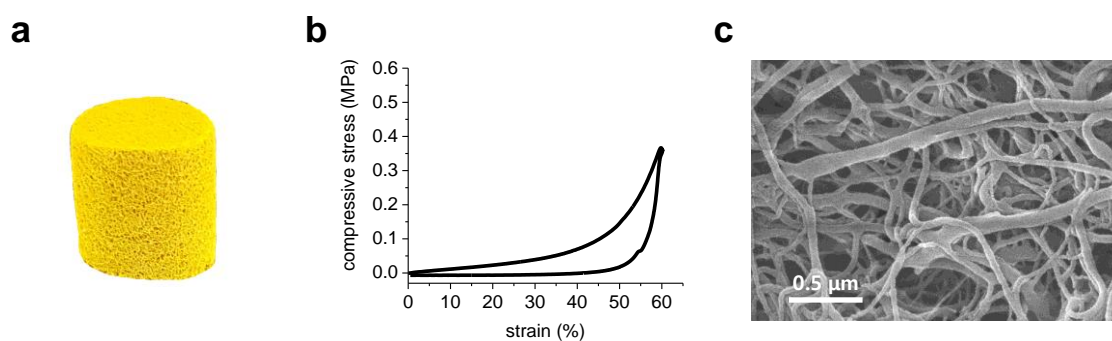


**Figure S1.** (a) Photographs of a cylindrical monolith based on the network **3** obtained from 1:1 PhMe–THF (0.3 M). (b) Compressive stress–strain curve obtained from the material (diameter, 8 mm; height, 5 mm) and (c) its SEM image measured at the magnification of 50,000 $\times$ .

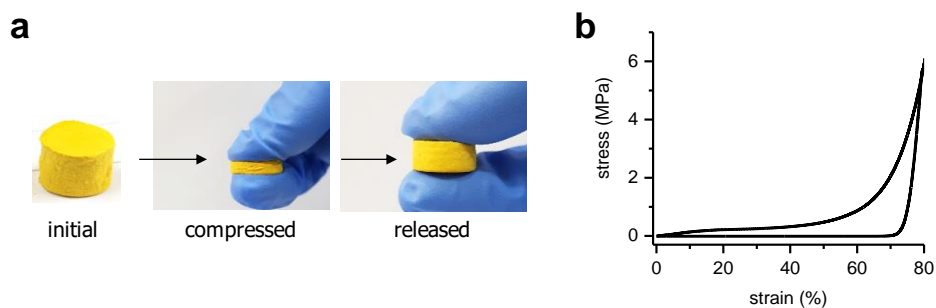


**Figure S2.** (a) Photographs for the initial cylindrical monolith **3** (diameter, 7 mm; height, 6 mm) (left) and that when compressed by hand (middle) and after released (right). (b) The measured stress–strain curve of **3** in a compressive mode. A cylindrical sample measured has also the same size as that shown in left.

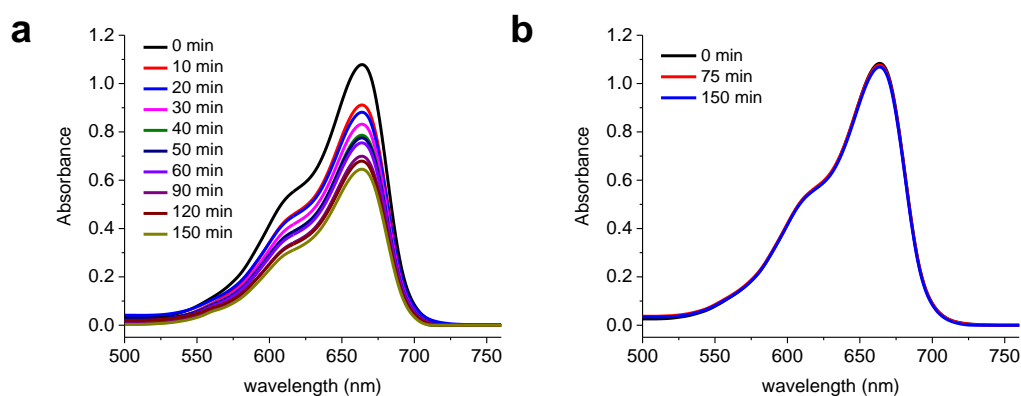


**Figure S3.** Representative absorption spectra of the solution of methylene blue in 4:1 water–methanol (4 ppm) during the control degradation reaction without (a) the light irradiation or (b) the film, when observed at specific time intervals.

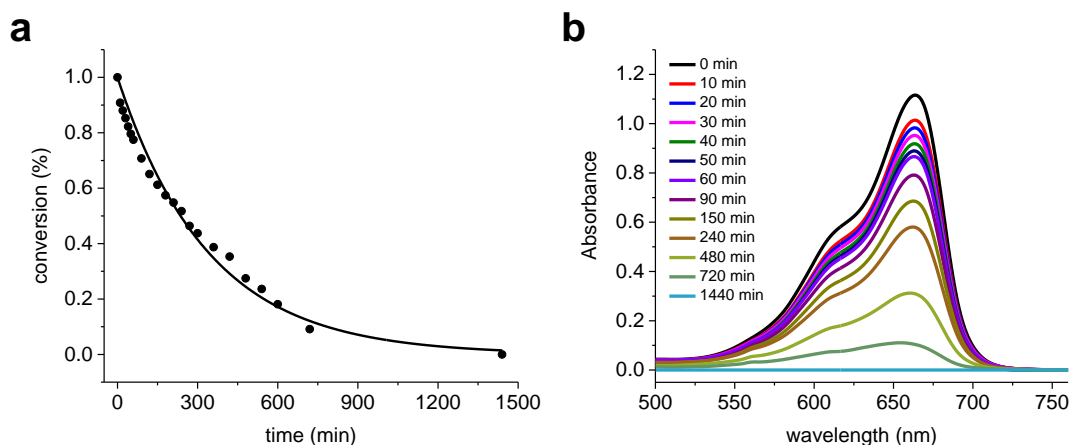


**Figure S4.** (a) Change in the concentration of the solution of methylene blue in 4:1 water–methanol (4 ppm) in the presence of the cylindrical sample (14.2 mg) from **3** under white light irradiation. (b) The representative absorption spectra obtained at different time intervals during the degradation reaction.

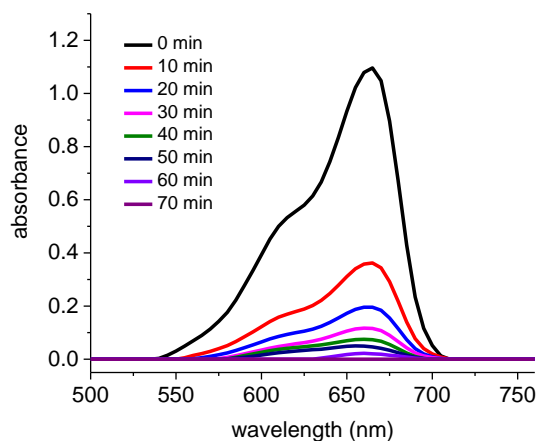


**Figure S5.** Representative absorption spectra of the methylene blue solution (4 ppm) during the degradation reaction in the presence of the powdery sample (14.2 mg) under white light irradiation.

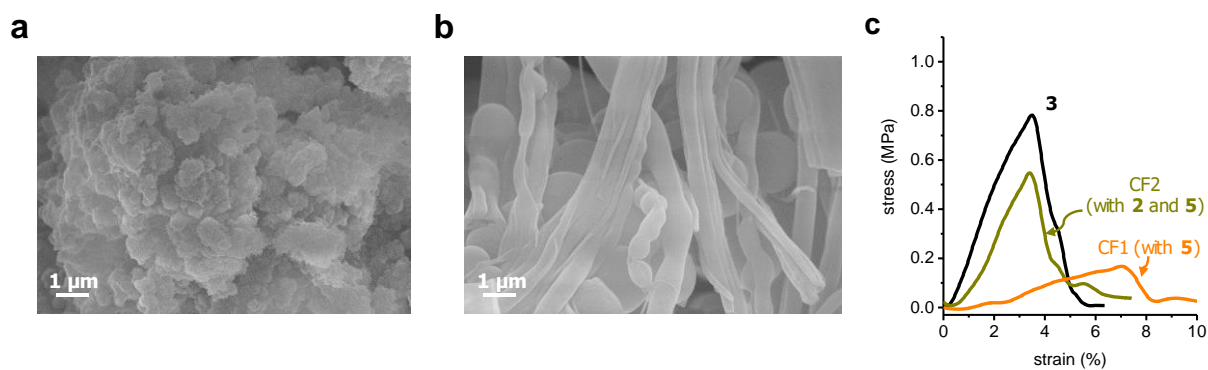


**Figure S6.** (a, b) The obtained SEM images of CF1 prepared with **5** (a) or CF2 prepared with the 1:1 mixture of **2** and **5** (b) when measured at the magnification of 10,000 $\times$ . (c) The measured tensile stress–strain curves of CF1 (orange) or CF2 (olive). The tensile curve of **3** is shown for comparison (black).

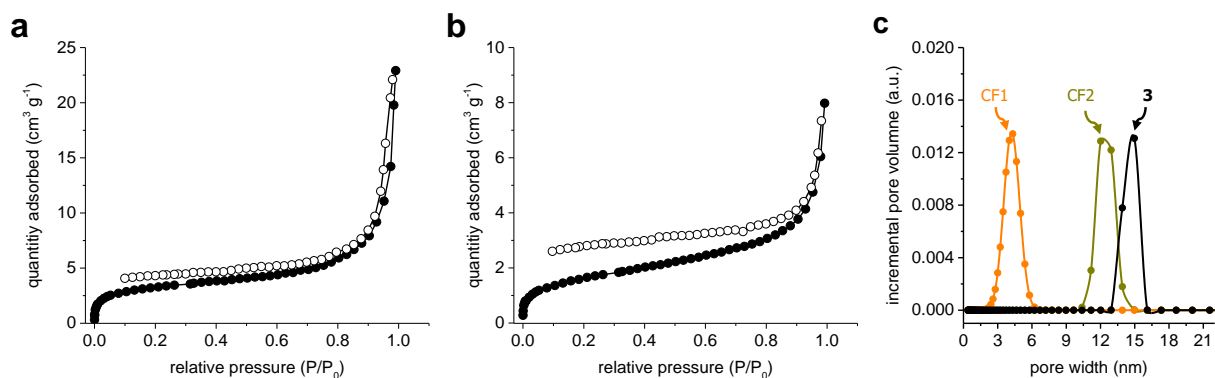


**Figure S7.** (a, b) Nitrogen adsorption–desorption isotherms of CF1 prepared from **5** (a) or CF2 from the 1:1 mixture of **2** and **5** (b) when measured at 77 K. Closed circles indicate adsorption; open circles, desorption. (c) The estimated NLDFT pore size distributions of CF1 (orange) or CF2 (olive). The data points for **3** is shown for comparison (black).

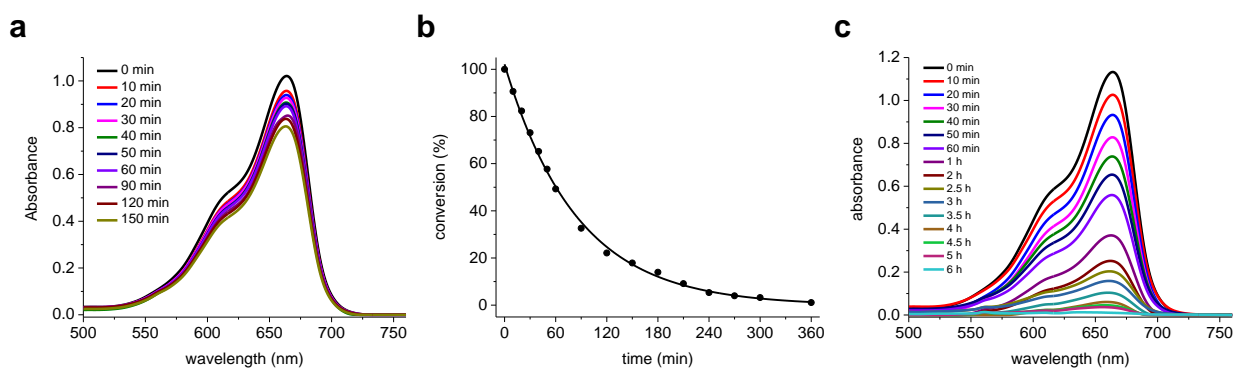


**Figure S8.** (a) Representative absorption spectra of the methylene blue solution (4 ppm) during the degradation reaction, when measured at different time intervals in the presence of CF1 under white light irradiation. (b) Change in the concentration of the methylene blue solution (4 ppm) during the degradation reaction over the course of 6 h in the presence of CF2 under white light irradiation. (c) The obtained representative absorption spectra of the methylene blue solution during the degradation reaction using CF2 under the irradiation.

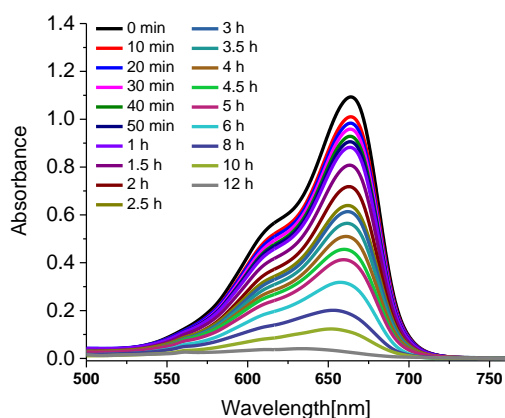


**Figure S9.** Representative absorption spectra of the methylene blue solution (4 ppm) during the degradation reaction, when measured at different time intervals in the presence of CF3 prepared from **4** and **2** (14.2 mg) under white light irradiation.

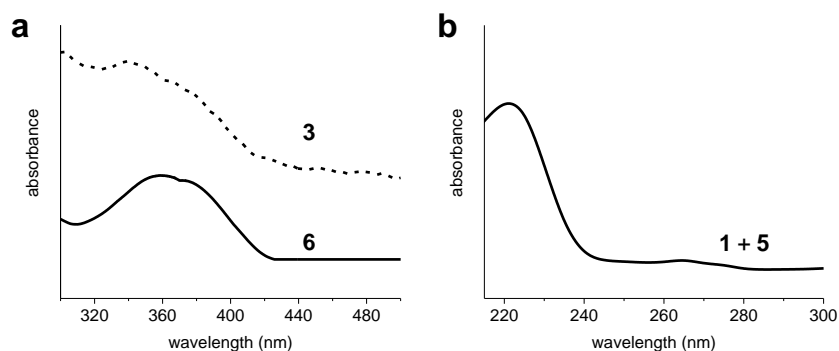


**Figure S10.** (a) Comparison of the absorption spectra of the network **3** (dashed) and the model compound **6** (solid). (b) The obtained spectra of the control network obtained from **1** and **5**.

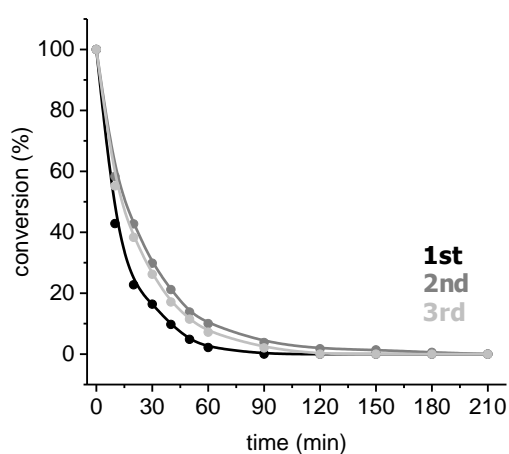


**Figure S11.** Change in the concentration of the methylene blue solution (4 ppm) during three repeating cycles of the photocatalytic degradation reaction using the same film (14.2 mg) prepared from **3**.

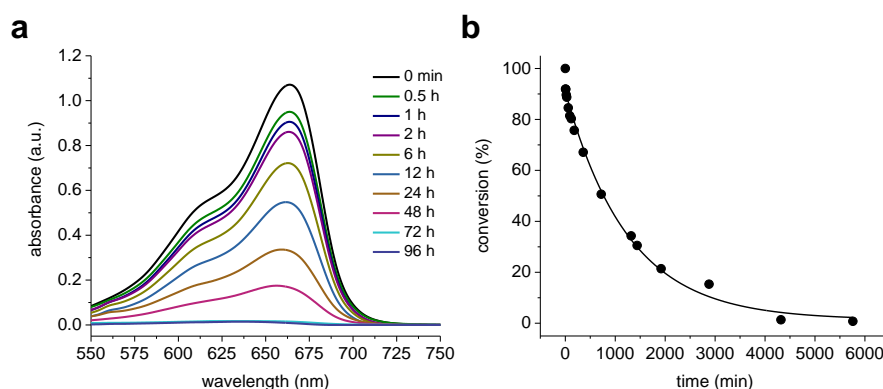


**Figure S12.** (a) Representative absorption spectra of the methylene blue solution (4 ppm) during the degradation reaction, when measured at different time intervals in the presence of **6** under white light irradiation. (b) Change in the concentration of the methylene blue solution (4 ppm) during the degradation reaction over the course of 96 h in the presence of **6** under white light irradiation.

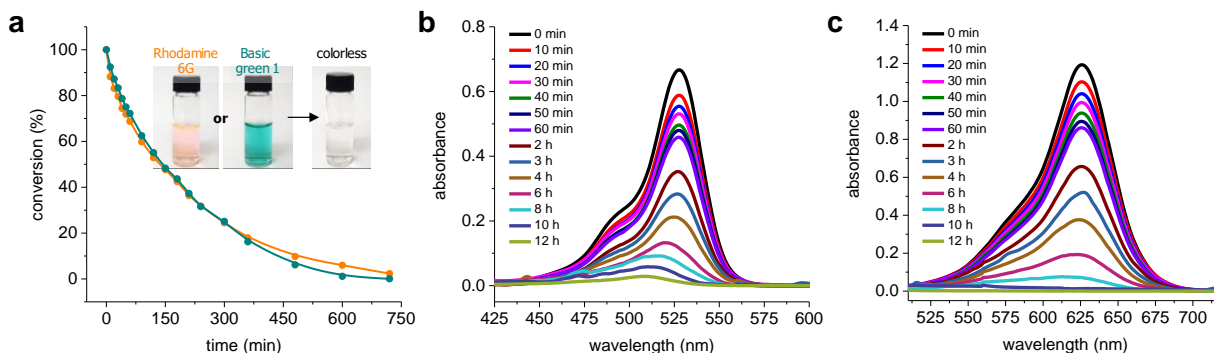


**Figure S13.** (a) Change in the concentrations of other aromatic dyes such as rhodamine 6G (orange) and basic green 1 (olive) (4 ppm, each) in 4:1 water–methanol when degraded under white light irradiation in the presence of the film from **3** (14.2 mg). The insets show each solution of the dye that turned to transparent after the reaction. (b and c) Representative spectra of the solutions of (b) rhodamine 6G and (c) basic green 1 during the photocatalytic degradation when measured at specific time intervals under white light irradiation.

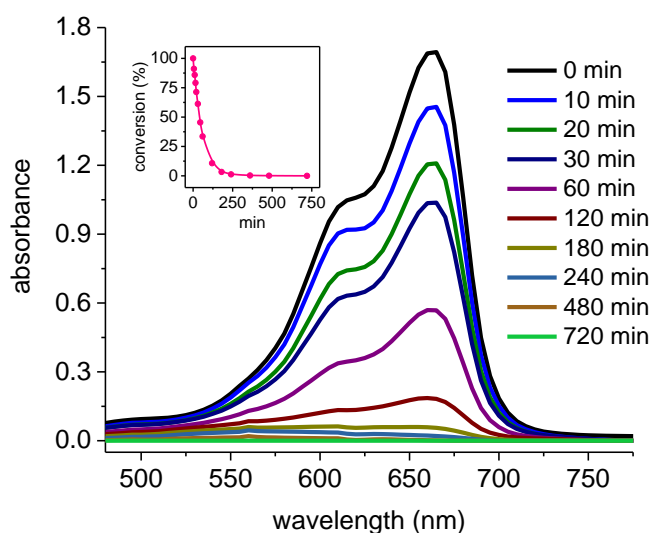


**Figure S14.** Representative absorption spectra of the solution of methylene blue during the oxidative degradation reaction using Oxone® (40 mg) when measured at specific time intervals. The inset shows the change in the concentration of the dye solution.



## NMR and HRMS Spectra

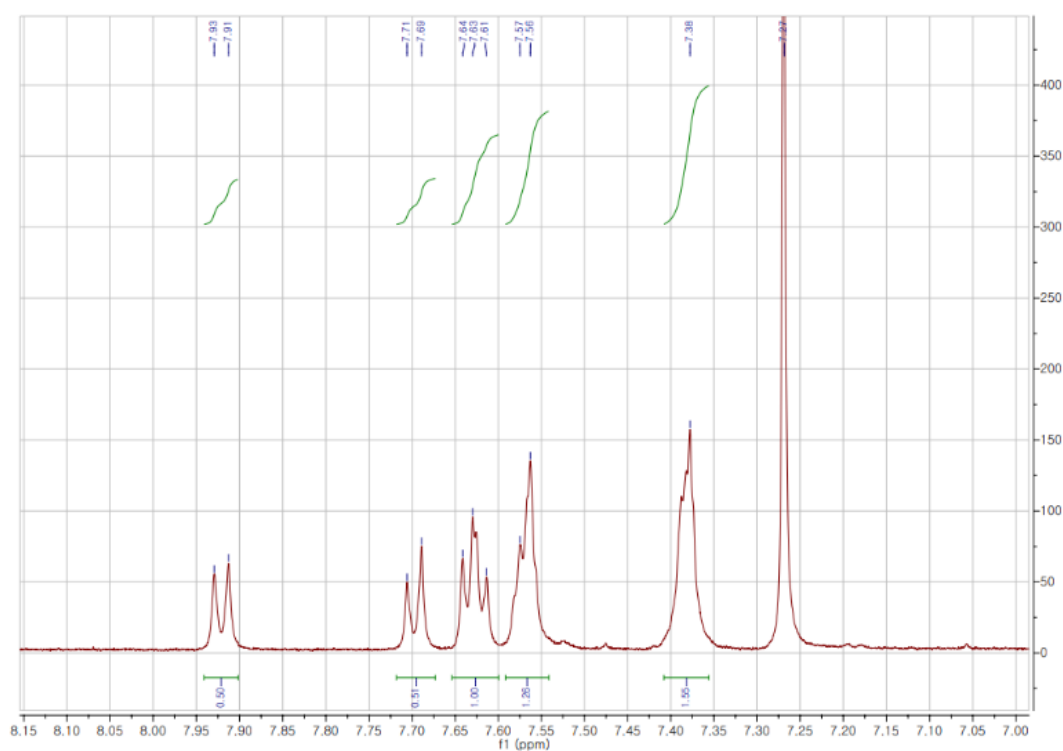


Figure S15.  $^1\text{H}$  NMR spectrum of 6.

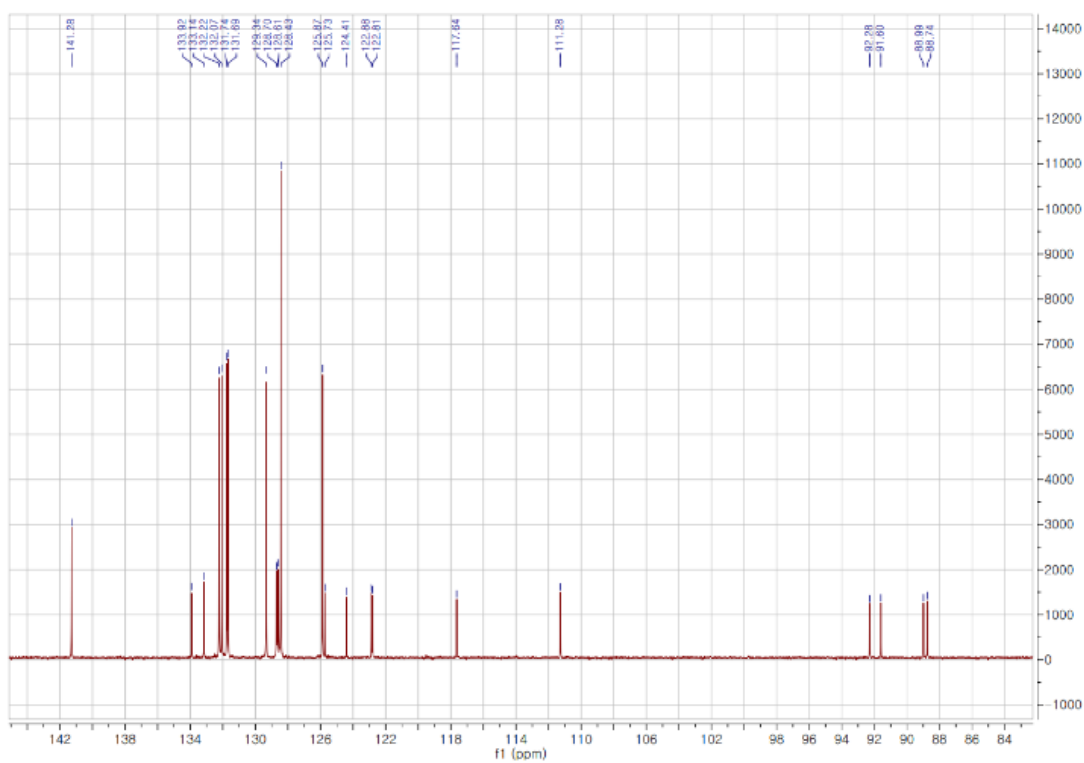


Figure S16.  $^{13}\text{C}$  NMR spectrum of 6.

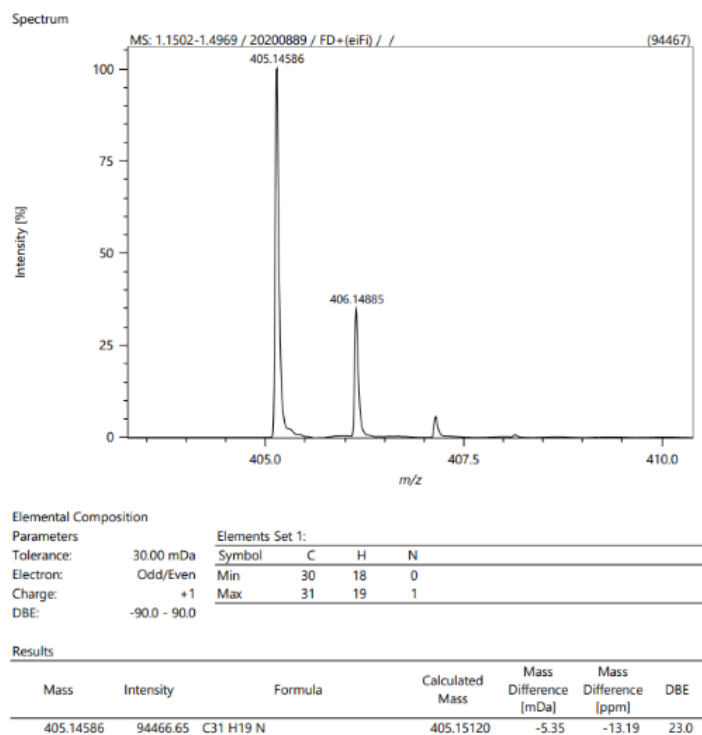


Figure S17. HRMS spectrum of 6.

## References

- [S1] A. Galanti, V. Diez-Cabanes, J. Santoro, M. Valášek, A. Minoia, M. Mayor, J. Cornil, P. Samorì, *J. Am. Chem. Soc.* **2018**, *140*, 16062–16070.
- [S2] C.-H. Chen, S.-L. Lee, T.-S. Lim, C.-H. Chen, T.-Y. Luh, *Polym. Chem.* **2011**, *2*, 2850–2856.
- [S3] J. A. Chae, Y. Oh, H. J. Kim, G. B. Choi, K. M. Lee, D. Jung, Y. A. Kim, H. Kim, *Polym. Chem.* **2019**, *10*, 5142–5150.